



# Surface interactions, thermodynamics and topography of binary monolayers of Insulin with dipalmitoylphosphatidylcholine and 1-palmitoyl-2-oleoylphosphatidylcholine at the air/water interface



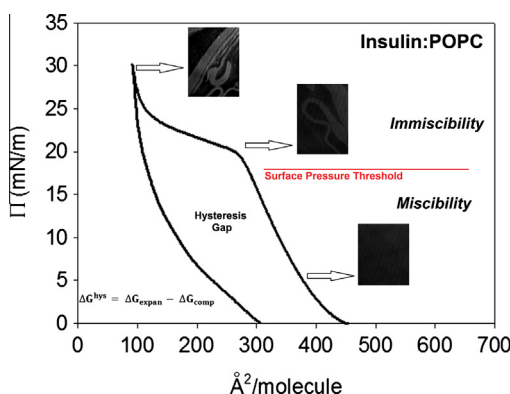
E.J. Grasso\*, R.G. Oliveira, B. Maggio

CIQUIBIC, Universidad Nacional de Córdoba–CONICET, Departamento de Química Biológica, Facultad de Ciencias Químicas, Universidad Nacional de Córdoba, Argentina

## HIGHLIGHTS

- Insulin forms non-ideal, stable films with DPPC and POPC.
- Under compression the films exhibit a viscoelastic or kinetically trapped organization.
- Hysteresis of films under expansion occurs with entropic–enthalpic compensations.
- BAM reveals domain coexistence at relatively high  $\Pi$  showing a striped appearance.

## GRAPHICAL ABSTRACT



## ARTICLE INFO

### Article history:

Received 4 September 2015  
Revised 15 November 2015  
Accepted 17 November 2015  
Available online 19 November 2015

### Keywords:

Langmuir monolayers  
Insulin  
Dipalmitoylphosphatidylcholine (DPPC)  
1-Palmitoyl-2-oleoylphosphatidylcholine (POPC)  
Binary monolayers  
Insulin surface behavior  
Hysteresis

## ABSTRACT

The molecular packing, thermodynamics and surface topography of binary Langmuir monolayers of Insulin and DPPC (dipalmitoylphosphatidylcholine) or POCP (1-palmitoyl-2-oleoylphosphatidylcholine) at the air/water interface on  $Zn^{2+}$  containing solutions were studied. Miscibility and interactions were ascertained by the variation of surface pressure–mean molecular area isotherms, surface compressional modulus and surface (dipole) potential with the film composition. Brewster Angle Microscopy was used to visualize the surface topography of the monolayers. Below 20 mN/m Insulin forms stable homogenous films with DPPC and POCP at all mole fractions studied (except for films with  $X_{INS} = 0.05$  at 10 mN/m where domain coexistence was observed). Above 20 mN/m, a segregation process between mixed phases occurred in all monolayers without squeezing out of individual components. Under compression the films exhibit formation of a viscoelastic or kinetically trapped organization leading to considerable composition-dependent hysteresis under expansion that occurs with entropic–enthalpic compensation. The spontaneously unfavorable interactions of Insulin with DPPC are driven by favorable enthalpy that is overcome by unfavorable entropic ordering; in films with POCP both the enthalpic and entropic effects are unfavorable. The surface topography reveals domain coexistence at relatively high pressure showing a striped appearance. The interactions of Insulin with two major membrane phospholipids induces composition-dependent and long-range changes of the surface organization that ought to be considered in the context of the information-transducing capabilities of the hormone for cell functioning.

© 2015 Elsevier Inc. All rights reserved.

\* Corresponding author at: Laboratorio de Bioquímica y Biología Reproductiva, ICTA–Facultad de Ciencias Exactas, Físicas y Naturales, e IIBYT, CONICET–Universidad Nacional de Córdoba, Av. Velez Sarsfield 1611, CP: 5016 Córdoba, Argentina.

E-mail address: [ejgrasso@conicet.gov.ar](mailto:ejgrasso@conicet.gov.ar) (E.J. Grasso).

## 1. Introduction

Insulin is a polypeptide hormone (MW ~5800 Da) composed of two peptide chains linked by disulfide bridges differing in their hydrophobicity and charge at physiological pH [6,29]. The hormone is synthesized and stored in  $\beta$  cells of the pancreas as a biologically inactive  $\text{Zn}^{2+}$ -linked hexamer [10]. When released into the bloodstream, the hexamers dissociates into dimers and subsequently into biologically active monomers [15] facilitating glucose transport into cells by at least two different steps: binding to a membrane receptor followed by activation of a glucose transporter [14,22,34]. The Insulin monomer is unstable and tends to macroscopically aggregate in aqueous solutions during storage [16,13,6]. This is a consequence of solid fibers formed by aggregation of monomers and dimers under low pH conditions [32,30]; and causes loss of hormone biological activity which is a major obstacle for developing long-term delivery formulations. Though the mechanism of aggregation of Insulin still remains unclear, some studies suggested that the presence of different hydrophobic environments (i.e. air/water or lipid/water interfaces) may be involved in the formation of aggregates [23] that may avoid gastrointestinal peptidases [11]. In any way, surface interactions will be of importance in any effect derived from aggregation or interactions of the hormone with cell membranes.

Insulin Langmuir monolayers at the air/water interface were previously described under different experimental conditions such as pH, temperature and ion concentration [29,32,24]. Also, it has been recently shown that the presence of  $\text{Zn}^{2+}$  has a profound effect on the surface behavior of Insulin monolayers [32,24,20]. We recently described the rheological properties of regular Insulin and aspart Insulin in presence on  $\text{Zn}^{2+}$ . By oscillatory compression–expansion cycles, we observed in all Insulin monolayers the development of a dilatational response to the surface perturbation, exhibiting a well-defined shear moduli in the presence of  $\text{Zn}^{2+}$ , which was higher for regular Insulin compared to aspart Insulin. Development of a shear modulus indicates behavior resembling a nominal solid, suggesting formation of viscoelastic networks at the surface [20].

Besides the receptor-mediated function of the hormone, it is important to understand its possible effects on cell membranes. The works by Pérez-López et al. using natural phospholipid mixtures represents a pioneering step in that regard [31,32]. These authors have described the behavior of binary monolayers of Insulin–sphingomyelin and Insulin–egg phosphatidylcholine (PC) at the air/water interface on pure water, NaOH and phosphate-buffered solutions of pH 7.4, and on  $\text{Zn}^{2+}$ -containing solutions [32,31]. Their results indicated that intermolecular interactions between Insulin, sphingomyelin and egg-PC depend on both the monolayer state and the structural characteristics of Insulin at the interface, which are strongly influenced by the subphase pH and salt content.

The natural phospholipids used in those studies consist of heterogeneous mixtures of many phospholipid species, each of them possibly having different interactions with the protein, while the molecular interactions of Insulin with well defined, single species of phospholipids has not, as far we know, been explored. Comprehension of specific molecular interactions of Insulin with defined phospholipids, and their longer-range consequences on the surface organization is necessary in order to further understanding of such effects. With this aim, we studied in this work the surface behavior of mixed films of Insulin with DPPC and POPC, two major and well characterized constituents of egg and natural PCs, on  $\text{Zn}^{2+}$  containing solutions (where Insulin molecules form hexamers showing well defined organization states and interesting viscoelastic properties [29,24,20]). Besides classical miscibility

studies, we focused on the thermodynamics of the mixing process, on the presence of monolayer hysteresis and on exploring the surface topography of the films by Brewster Angle Microscopy. Our results reveal novel features of the surface organization and thermodynamics of these binary interfaces that may also have some implications for the stability of possible formulations and for the construction of nanofilms as supports for stimulated cellular growth. In this connection, we have previously shown that surfaces coated with Insulin, in presence of  $\text{Zn}^{2+}$ , selectively influence hippocampal neuron polarization depending on the molecular organization of the Insulin film on which cells are grown; this indicated that recognition events mediated by different molecular organizations of an Insulin-coated surface can finely mediate and modulate neuronal differentiation [21].

## 2. Materials and methods

### 2.1. Reagents

Bovine Insulin (MW 5733 Da) was purchased from Sigma–Aldrich, St Louis, MO, USA. DPPC and POPC were purchased from Avanti Polar Lipids, USA. Aqueous subphases were prepared with ultrapure water produced by a Millipore water purification system. NaCl and  $\text{ZnCl}_2$  were provided by Merck (Darmstadt-Germany). The surface tension and resistivity of the ultra-pure water used were 18.2 M $\Omega$  cm and 72.2 mN/m at 24 °C, respectively.

### 2.2. Insulin-DPPC/POPC binary monolayers

#### 2.2.1. Compression isotherms

Absence of surface active impurities before spreading the monolayers or in the spreading solvents was routinely checked [21] by reducing the initial trough area to about 10% of the initial area in the absence of spread Insulin-DPPC or POPC or by spreading 50  $\mu\text{L}$  of pure solvents; the changes in surface pressure ( $\Pi$ ) and surface potential were less than  $\pm 1.0$  mN/m and  $\pm 30$  mV, respectively. Stock solution of Insulin (14 mg/mL) were dissolved in ultrapure water –0.06 M HCl (pH = 2.5) [29]. DPPC or POPC were dissolved in chloroform:methanol (2:1). Spreading solutions of Insulin (0.125 nmol/ $\mu\text{L}$ ) were freshly prepared daily by adding the required amount of Insulin in water solution to the solvent solution (chloroform:methanol, 2:1 v/v) so that the proportions reached the ratio chloroform:methanol:water (60:30:4.5 v/v/v) which allows the system to remain in a single homogenous phase [18]; compression isotherms of Insulin spread from water [21] or from fresh solvent solutions were indistinguishable. Langmuir monolayers were formed onto the aqueous subphase (NaCl 145 mM plus  $\text{ZnCl}_2$  1 mM, pH 6.3) by spreading 25  $\mu\text{L}$  of Insulin–lipid premixed solvent solutions (0.16–1.11 nmol/ $\mu\text{L}$ ) in the desired proportions. The protein and lipid concentrations were adjusted so that mixing of aqueous and solvent solutions were always kept within the proportions maintaining the final solution in a single homogeneous phase [18]. We waited 10 min for solvent evaporation and monolayer equilibration before compression. Isothermic compression and decompression isotherms (speed = 20  $\text{\AA}^2/\text{molecule}/\text{min}$ ), were carried out in a KSV-minitrough, having a Teflon trough with a surface area of 266  $\text{cm}^2$  and a Wilhelmy-Pt plate surface pressure sensor and two symmetrically moving barriers. The temperature was maintained at  $24 \pm 0.5$  °C with an external circulating water bath (Haake F3C). The collapse pressure, surface pressure point for molecular reorganization and limiting mean molecular area of the Insulin films were determined from the third derivative of the compression isotherms [8], after being reproduced in at least three independent experiments.

### 2.2.2. Surface potential

Surface potential measurements were performed with a vibrating plate (capacitor like system, KSV Instruments Ltd., Helsinki, Finland). The resultant perpendicular dipole moment of Insulin is directly proportional to the surface (dipole) potential per unit of molecular surface density  $[\Delta V/n = \Delta V \cdot \text{MMA}]_{II}$  where  $n$  is the density of overall molecular dipoles in the film (the inverse of the mean molecular area, MMA) at a defined surface pressure [19,7].

### 2.2.3. Surface compressional modulus

The surface compressional modulus,  $K^s$ , (in-plane elasticity) [7,9] of the mixed films was calculated directly from the surface pressure-mean molecular isotherm according to

$$K^s = -A \left( \frac{\partial \Pi}{\partial A} \right)_T \quad (1)$$

where  $A$  is the mean molecular area (MMA) and  $\Pi$  is the surface pressure.

### 2.2.4. Brewster Angle Microscopy

For film imaging, Brewster Angle Microscopy (BAM) was performed with an autonulling imaging ellipsometer (Nanofilm EP3SE, Accurion GmbH, Germany) equipped with a 532 nm laser, 10× and 20× objectives, and a CCD camera. By using p-polarized light, we measured the Reflectivity<sub>p</sub>,  $R_p = \frac{I_p}{I_{0p}}$ , where  $I_p$  is the reflected light intensity and  $I_{0p}$  is the incoming p-polarized beam intensity.

### 2.2.5. Thermodynamic functions of hysteresis

In ideally fluid films hysteresis is absent,  $\Delta G_i^{\text{hys}} = 0$ ,  $\Delta S_i^{\text{hys}} = 0$  and  $\Delta H_i^{\text{hys}} = 0$ . The free energy of hysteresis  $\Delta G^{\text{hys}}$ , the configurational entropy of hysteresis  $\Delta S^{\text{hys}}$  and the enthalpy of hysteresis  $\Delta H^{\text{hys}}$  are defined by Eqs. (2)–(5), respectively [5]:

$$\Delta G^{\text{hys}} = \Delta G_{\text{expan}} - \Delta G_{\text{comp}} \quad (2)$$

$$\left[ \Delta S_{II}^{\text{hys}} = R \ln \frac{A_{\text{expan}}}{A_{\text{comp}}} \right]_{II} \quad (3)$$

$$\Delta S^{\text{hys}} = \sum_{II} \Delta S_{II}^{\text{hys}} \quad (4)$$

$$\Delta H^{\text{hys}} = \Delta G^{\text{hys}} + T \Delta S^{\text{hys}} \quad (5)$$

For the thermodynamic functions of hysteresis, the difference is taken between the values of expansion and those of compression. Reducing the barrier speed by half did not affect the compression–expansion isotherms nor the hysteresis.

### 2.2.6. Thermodynamic functions of mixing

The free energy of mixing for a binary monolayer ( $\Delta G_{\text{mix}}$ ) is derived from the subtraction of the ideal free energy of mixing ( $\Delta G_{\text{mix}}^i$ ) and the measured excess free energy of mixing ( $\Delta G_{\text{mix}}^{\text{exc}}$ ) [5]. The excess free energy of mixing is computed as the difference between the integral area under the experimental compression  $\Pi$ -area isotherms of a given mixture and the integral area under the ideally mixed isotherm. The integration was taken between  $\Pi_1 = 1$  mN/m and  $\Pi_2 = 30$  mN/m. This avoids the rather variable gaseous region of the isotherm and irreproducible inconsistencies related to variation of the compressibility in films approaching collapse [5]. Thus, the excess free energy of mixing is expressed as:

$$\Delta G_{\text{mix}}^{\text{exc}} = \Delta G_{\text{mix}}^{\Pi \leq \Pi_c} - \Delta G_{\text{mix}}^i \quad (6)$$

### 2.2.7. Entropy of mixing for a binary monolayer

$\Delta S_{\text{mix}}$  is derived from the subtraction of the ideal entropy of mixing and the excess entropy of mixing [5]. The ideal entropy of mixing  $\Delta S_{\text{mix}}^i$  is:

$$\Delta S_{\text{mix}}^i = -R(X_1 \ln X_1 + X_2 \ln X_2) \quad (7)$$

where  $X_1$  and  $X_2$  are the mole fractions of components 1 and 2; by assuming that the excess entropy of mixing  $\Delta S_{\text{mix}}^{\text{exc}}$  is due solely to configurational entropy ( $\Delta S_{\text{mix}}^{\text{exc}} = \Delta S_{\text{cf}}^{\text{exc}}$ ) resulting from the isothermal area condensation/expansion [2]. It can be derived [1] from the measured mean molecular areas of experimental and ideal isotherms as:

$$\left[ \Delta S_{\text{mix}}^{\text{exc}} = \sum_{II} R \ln \frac{A_m}{A_i} \right]_{II, X} \quad (8)$$

$\Delta S_{\text{mix}}^{\text{exc}}$  for a mixture with a fixed proportion of components is represented by the sum of individual configurational entropy terms taken at discrete lateral pressure steps:

$$\Delta S_{\text{mix}}^{\text{exc}} = \sum_{II} [\Delta S_{\text{mix}}^{\text{exc}}]_{II} \quad (9)$$

From these, the entropic contribution to the excess free energy of mixing ( $T \Delta S_{\text{mix}}^{\text{exc}}$ ) can be obtained.

### 2.2.8. Enthalpy of mixing for a binary monolayer

$\Delta H_m$  is derived from the addition of the ideal enthalpy of mixing (equal to zero in an ideal mixture) and the experimental excess enthalpy of mixing,  $\Delta H_m^{\text{exc}}$ :

$$\Delta H_m = \Delta H_m^i + \Delta H_m^{\text{exc}} \quad (10)$$

The second term in Eq. (10) is obtained by adding the experimental values of excess free energy and the corresponding entropic contribution [5]:

$$[\Delta H_m^{\text{exc}} = \Delta G_m^{\text{exc}} + T \Delta S_m^{\text{exc}}]_X \quad (11)$$

The values of all thermodynamic parameters are interpreted within a “black-box” concept because several entropic contributions from different molecular factors are intrinsically included within the experimentally measured mean molecular area and its variations with film composition and surface pressure.

## 3. Results and discussion

### 3.1. Surface behavior of Insulin-DPPC/POPC binary monolayers in the presence of $\text{Zn}^{2+}$ in the subphase

The behavior at the air/water interface of pure Insulin in the presence of  $\text{Zn}^{2+}$  was previously described [29]. In the absence of  $\text{Zn}^{2+}$ , the predominant structure of Insulin in bulk phases at pH 2–8 is dimeric [29,24]; and, under such conditions, the protein maintains its ternary structure at 25 °C [24]. However, it is well known that this divalent cation can be incorporated into dimers, and it induces their association to form hexamers [24]. It has been previously described that upon spreading the protein on an aqueous  $\text{ZnCl}_2$  solution, stable hexamers are formed at the interface under monolayer compression [29]. Nevertheless, the two-dimensional mixing process and thermodynamics of Insulin with individual phosphatidylcholines with defined hydrocarbon chains, in presence of  $\text{Zn}^{2+}$ , had not been studied so far. Figs. 1–3 show surface pressure ( $\Pi$ ), surface potential ( $\Delta V$ ), surface potential per unit of molecular surface density ( $\Delta V/n$ ) and surface compression modulus ( $K^s$ ) recorded upon compression of films of pure Insulin, DPPC,

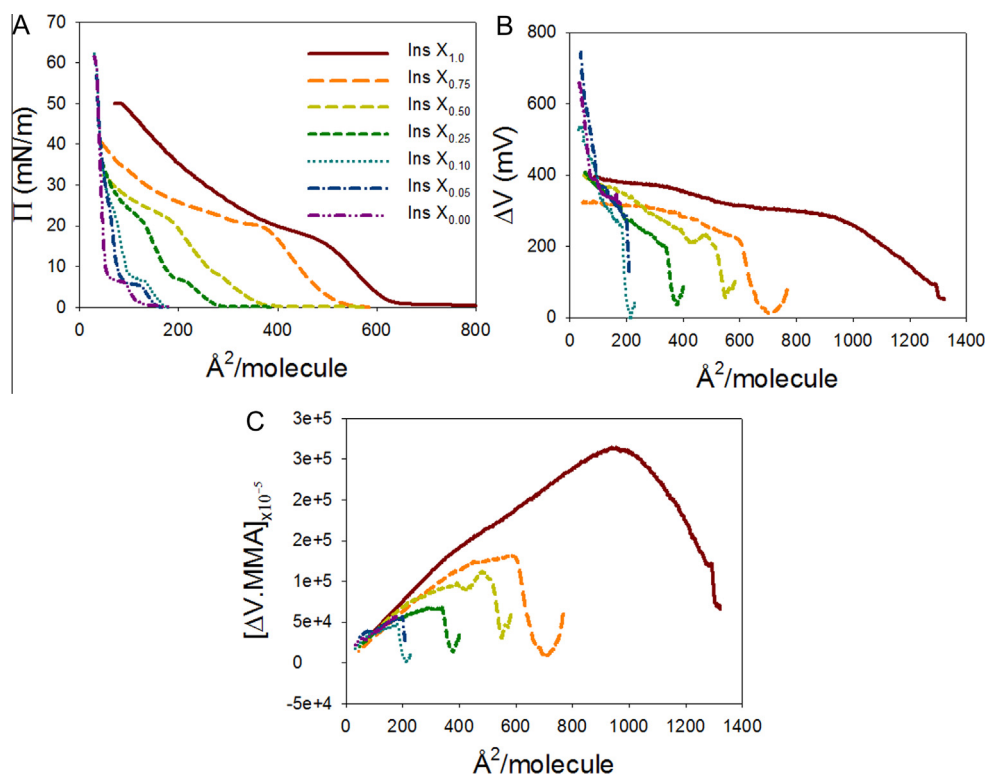


**Fig. 1.** Surface behavior of pure Insulin ( $X_1$ ), pure DPPC ( $X_0$ ) and their mixtures ( $X_{0.75-0.05}$ ). (A) Surface pressure. The lift off corresponds to a sectional MMA of  $\sim 700$ ,  $\sim 500$ ,  $\sim 370$ ,  $\sim 275$ ,  $\sim 165$ ,  $\sim 150$  and  $\sim 120 \text{\AA}^2/\text{molecule}$  for  $X_{\text{INS}}$  films: 1.0, 0.75, 0.50, 0.25, 0.10, 0.05 and 0.0, respectively, (B) surface potential, and (C) surface potential per unit of molecular surface density ( $[\Delta V.MMA]$ ). Compression speed was  $20 \text{\AA}^2/\text{molecule}/\text{min}$ .

POPC and of their mixtures in different mole fractions ( $X_{\text{INS}}$ ). The compression isotherms recorded for Insulin-DPPC monolayers shift to lower areas as the proportion of Insulin decreases (Fig. 1A). Pure Insulin monolayers undergo a surface pressure-induced reorganization under compression between MMA of about  $535 \text{\AA}^2/\text{molecule}$  (15 mN/m) and  $430 \text{\AA}^2/\text{molecule}$  (20 mN/m). Such reorganization was attributed to a reorientation of the hexamers [29,24]. The presence of  $\text{Zn}^{2+}$  considerably increases the  $K^s$  in both, the pre- and post-transition regions and causes a well-defined collapse at a MMA of  $\sim 150 \text{\AA}^2/\text{molecule}$  at  $\sim 55 \text{ mN/m}$  [29]. Pure DPPC monolayers at  $24^\circ\text{C}$  showed the usual lift-off at a MMA of  $\sim 90 \text{\AA}^2/\text{molecule}$ , the Le to Lc phase transition at  $\sim 6 \text{ mN/m}$  with a collapse pressure of about  $58 \text{ mN/m}$ . Similar to Insulin-DPPC binary monolayers, the compression isotherms recorded for binary Insulin-POPC monolayers shifted to lower areas as the proportion of Insulin decreases (Fig. 2A). Both Insulin-DPPC and Insulin-POPC showed a single collapse upon compression. Thus, no component was squeezed out of the films. As mentioned above, upon spreading the protein on an aqueous  $\text{ZnCl}_2$  solution, stable hexamers are formed at the interface under monolayer compression [29,24]. In this regard, neither pure Insulin nor binary monolayers showed the characteristic plateau due to the submersion of Insulin A chains into the subphase (when no  $\text{Zn}^{2+}$  is present); but showed an increase of the collapse pressure in all the mixtures [32]. These results agreed with the condensing effect of  $\text{Zn}^{2+}$  on the pure and binary Insulin monolayers, which is caused by an increasing of the proportion of hexamers and dimers, at the interface [32].

Figs. 1B and 2B shows the surface electrostatics of the monolayers. No fluctuations of the surface potential was observed before and after the lift off; such fluctuations suggest the presence of large patches of immiscible components in the monolayer [19]. A monotonic increase in  $\Delta V$  was observed for pure Insulin and its mixtures with both DPPC/POPC up to  $\sim 20 \text{ mN/m}$  in the composition range  $X_{\text{INS}} = 0.25-0.75$ . But, when the lipid proportion is increased

( $X_{\text{INS}} = 0.05-0.1$ ), a strong increase in  $\Delta V$  was observed. This result is logical, because lipid dipoles are better defined and oriented when compared to protein dipoles [19]. The surface potential measurements were standardized by calculating the variation with molecular packing of the surface potential per unit of molecular surface density,  $\Delta V/n$  (Figs. 1C and 2C). This parameter is correlated to changes of organization of the average resultant molecular dipole moment perpendicular to the interface and its variation under film compression. Several combined electrostatic contributions, which cannot be readily separated, are involved in this parameter [7]. Nevertheless its variations and deviations from the additivity rule is a sensitive indicator of the mixing process and of the film molecular organization. We will resume the analysis of  $\Delta V/n$  variations when analyzing the deviation from ideality of mean molecular area and the surface potential per unit of molecular surface density as function of the film composition.

The surface compressional modulus ( $K^s$ ) versus mean molecular area in Insulin-DPPC or Insulin-POPC binary monolayers (Fig. 3A and B) shows that all binary monolayers correspond to rather compressible states with values of  $K^s$  lower than  $90 \text{ mN/m}$ . The well-known Lc state ( $K^s$  higher than  $200 \text{ mN/m}$ ) was observed only for pure DPPC monolayers. Thus, the presence of Insulin in a condensed DPPC films at high  $\Pi$  involves formation of more liquid-expanded states as evidenced by a large decrease of  $K^s$  for all mixtures, suggesting the possibility of at least partial miscibility. This fact was not so apparent in Insulin-POPC binary monolayers because the pure monolayers had similar compressibilities.

To further examine the miscibility of the two components in the binary films, the analysis of critical  $\Pi$  values ( $\Pi_{\text{transition}}$  and  $\Pi_{\text{collapse}}$ ) of DPPC/POPC and Insulin films can be helpful because the variation of those surface pressures points with the film composition may reveal 2D miscibility [17]. Our results show a significant increase of Insulin  $\Pi_{\text{transition}}$  when mixing with DPPC (from  $14.5$  to  $23.3 \text{ mN/m}$ ,  $p < 0.05$  Student's  $T$  test); and small but steady increase

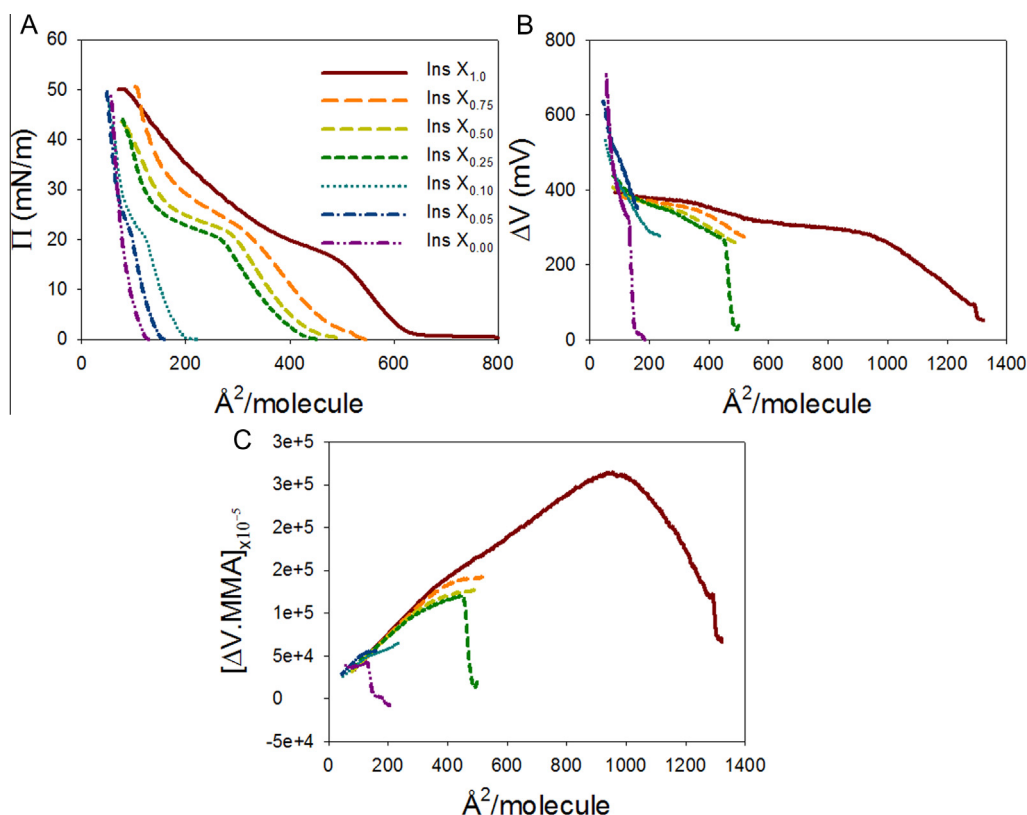


**Fig. 2.** Surface behavior of pure Insulin ( $X_1$ ), pure POPC ( $X_0$ ) and their mixtures ( $X_{0.75-0.05}$ ). (A) Surface pressure. The lift off corresponds to a sectional MMA of  $\sim 700$ ,  $\sim 520$ ,  $\sim 460$ ,  $\sim 420$ ,  $\sim 190$ ,  $\sim 140$  and  $\sim 120 \text{\AA}^2/\text{molecule}$  for  $X_{\text{INS}}$  films: 1.0, 0.75, 0.50, 0.25, 0.10, 0.05 and 0.0, respectively. (B) surface potential, and (C) surface potential per unit of molecular surface density ( $[\Delta V.MMA]$ ). Compression speed was  $20 \text{\AA}^2/\text{molecule}/\text{min}$ .

of  $\Pi_{\text{transition}}$  of both Insulin and DPPC in the mixed films up to  $X_{\text{INS}} 0.75$  where the DPPC- $\Pi_{\text{transition}}$  was absent (Fig. 3A) together with a significant decrease of  $\Pi_{\text{collapse}}$  over the composition range  $X_{\text{INS}} = 0.75-0.5$ . The  $\Pi_{\text{collapse}}$  of Insulin-POPC binary monolayers was reduced from  $\sim 50 \text{ mN/m}$  (pure Insulin) to  $32.8 \text{ mN/m}$  ( $p < 0.05$ , Student's  $T$  test) over the composition range  $X_{\text{INS}} = 0.75-0.25$ . However, at the lowest Insulin mole fraction, no significant differences of  $\Pi_{\text{collapse}}$  were observed when compared to pure DPPC and POPC, respectively. This demonstrates that at high surface pressures (after Insulin reorganization) the films behave ideally at  $X_{\text{INS}} = 0.1-0.05$ . As mentioned before, additional information can be obtained by analyzing the deviation from ideality of mean molecular area and the surface potential per unit of molecular surface density as function of the film composition. Fig. 5 shows MMA- $X_{\text{INS}}$  and  $\Delta V/n-X_{\text{INS}}$  plots at several  $\Pi$  corresponding to different monolayer states. If the two components are fully immiscible or ideally miscible, the variation of MMA and  $\Delta V/n$  versus  $X_{\text{INS}}$  should be linear according to the additivity rule. Deviations from linearity can indicate non-ideal behavior, miscibility or partial miscibility, as well as some sort of molecular interactions [19]. Furthermore, direct visualization of the monolayer surface may be confirmatory of the existence of a de-mixing process (we will discuss this issue in the BAM section). We observed both positive (expansion) and negative (condensation) deviations from the additivity rule, with the magnitude of the deviations depending on the monolayer composition and surface pressure. This fact suggest that, at least a partial miscibility occurs in Insulin-DPPC and Insulin-POPC binary monolayers at defined proportions and surface pressures. Interestingly, we observed two well defined trends for deviations: before and after the surface pressure point ( $15-20 \text{ mN/m}$ ) for Insulin reorganization for both MMA and  $\Delta V/n$  versus  $X_{\text{INS}}$  (see Fig. 5). Insulin-DPPC binary monolayers showed generally negative deviations in MMA vs

$X_{\text{INS}} = 0.75-0.25$  being larger after Insulin reorganization. These phenomena occurred with a hyperpolarization of the films being maximal at  $20 \text{ mN/m}$  at  $X_{\text{INS}} = 0.75$ . However, for mixed Insulin-POPC monolayers, an expansion of the MMA and hyperpolarization at  $X_{\text{INS}} = 0.75-0.25$  were observed before Insulin reorganization. It is important to remark that in mixtures with DPPC it is likely that over the composition range of  $X_{\text{INS}} = 0.5-0.05$ , and at surface pressures of  $25 \text{ mN/m}$  and above, there may be immiscibility between a highly lipid enriched mixture and a lipid-protein mixture with different proportions of protein; for POPC the situation is similar although the variation of the surface potential per unit of molecular surface density ( $\Delta V.MMA$ ) with composition reduces the immiscibility range to  $X_{\text{INS}} = 0-0.1$  or  $0.2$ . At high surface pressures ( $>20 \text{ mN/m}$ ) and at low Insulin mole ratio ( $X_{\text{INS}} = 0.1-0.05$ ) the system behaves ideally for both Insulin-DPPC/POPC, similar to  $\Pi_{\text{collapse}}$  described above. This suggests immiscibility or a de-mixing process, but no squeezing out of any pure component was observed during the compression isotherms (see Figs. 1A and 2A). Then, although a de-mixing process appears to be present, it is likely that immiscibility is established among mixtures of components in different proportion. Nevertheless, these films seems to be in a thermodynamically trapped and relatively long-lived metastable state (we will further address this issue in the hysteresis section).

It has been proposed that insulin hexamers undergo a change of orientation upon film compression in a way that the polar region of the oligomers become more submerged in the subphase [32]. In such states, these ternary structures should occupy less area at the interface as suggested by the values of MMA at the beginning and the end of the pressure range for the protein reorganization (Fig. 1A). In Insulin-DPPC binary films, the likely change of hexamer orientation would occur at pressures higher than  $15 \text{ mN/m}$  (see Figs. 1A and 3A). Pérez-López et al. [32] showed that

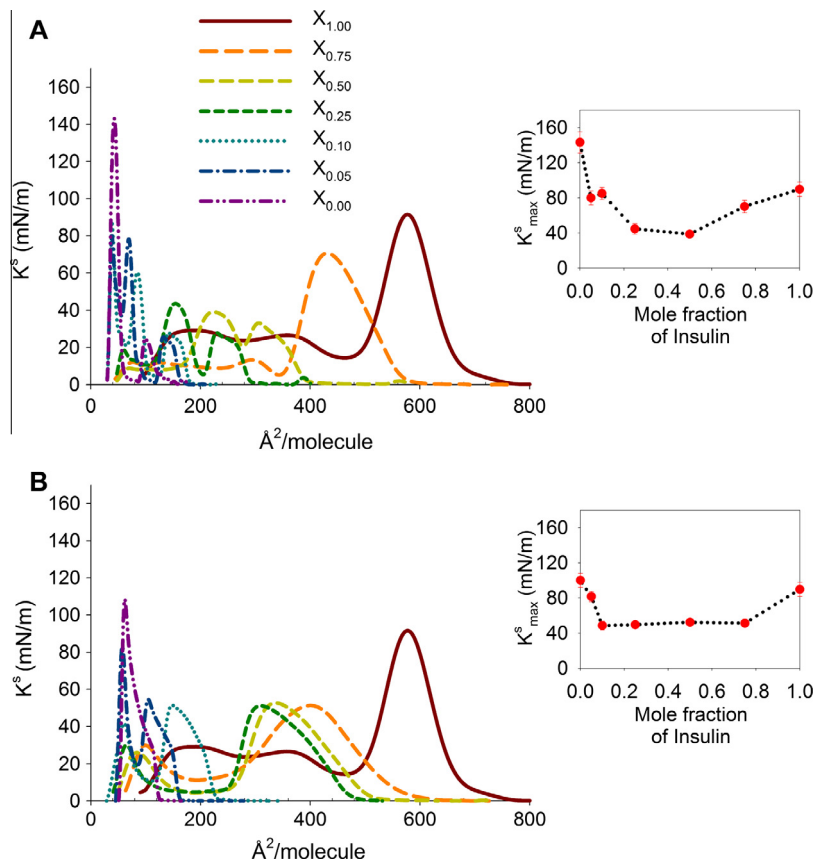


**Fig. 3.** Surface compressional moduli,  $K^s$ , as a function of the mean molecular area (MMA). (A) Insulin-DPPC binary monolayers. (B) Insulin-POPC binary monolayers. Compression speed was  $20 \text{ \AA}^2/\text{molecule}/\text{min}$ . Inset: maximum  $K^s$  values of pure components and their mixtures. Average values  $\pm$  SEM are result of three independent experiments.

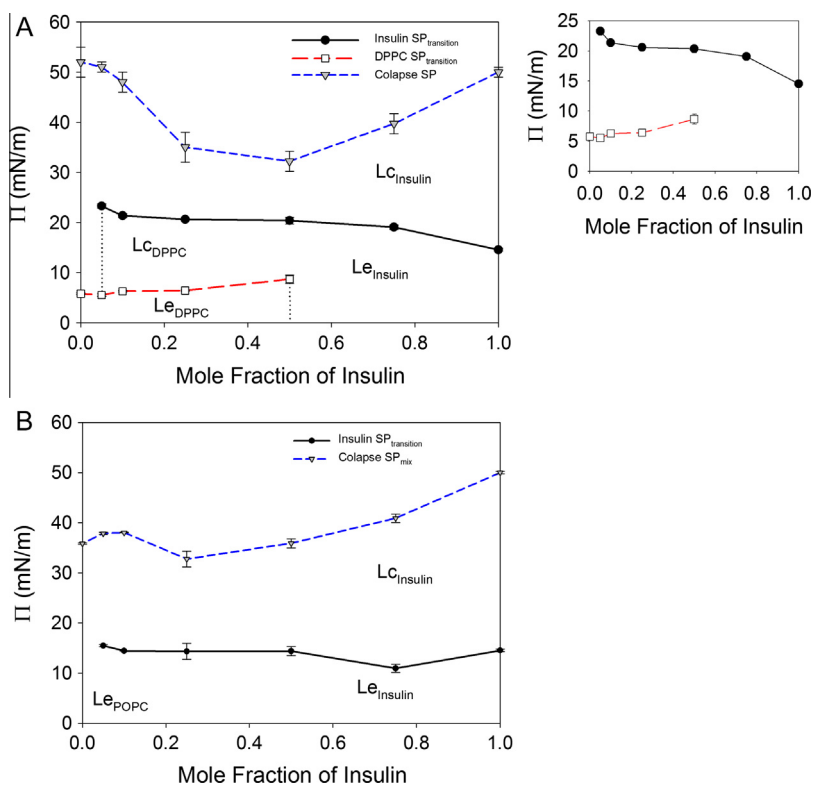


**Fig. 4.** (A) Two-dimensional pressure-composition phase diagram of Insulin-DPPC binary monolayers. (B) Idem for Insulin-POPC binary monolayers.

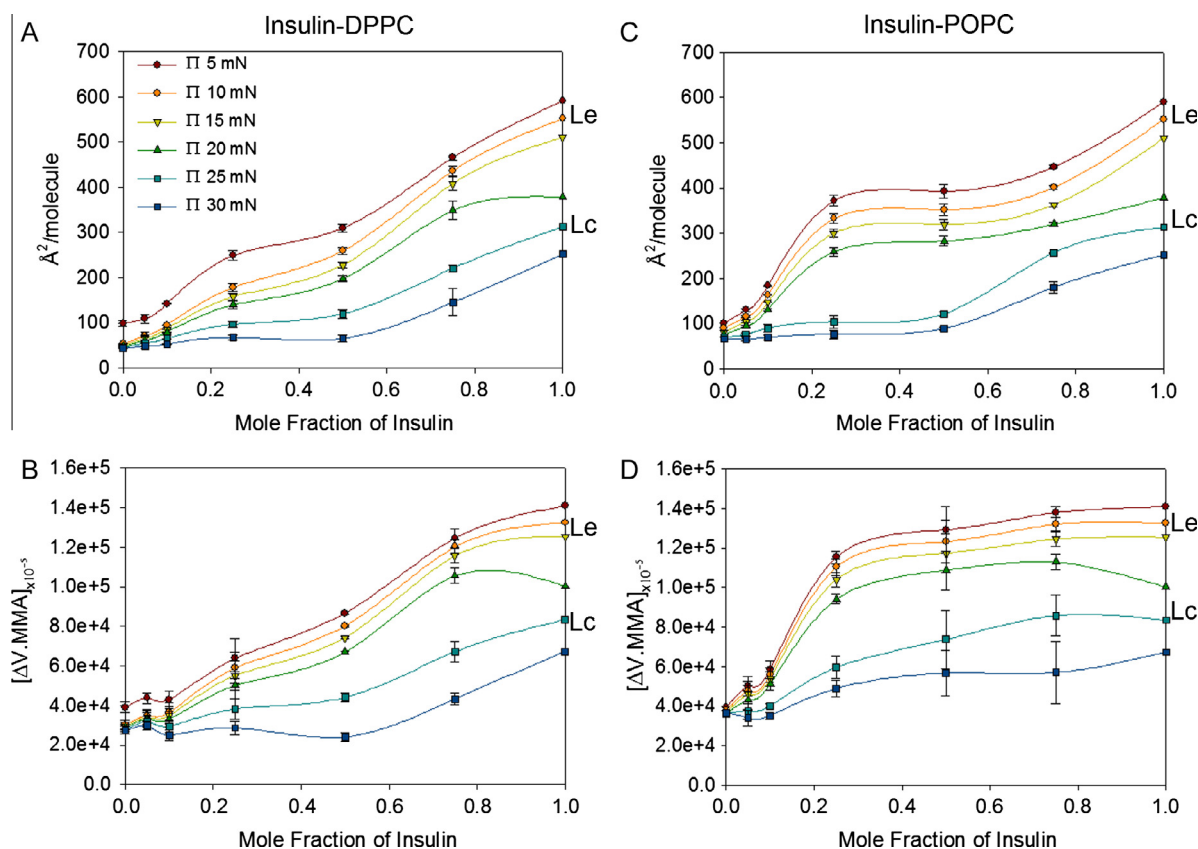


**Fig. 5.** (A and C) plots of mean molecular area as a function of the mole fraction of Insulin at different surfaces pressures (5–30 mN/m) for Insulin-DPPC and Insulin-POPC monolayers, respectively. (B and D) plots of the surface potential per unit of molecular surface density as function of mole fraction of Insulin. Le and Lc mean liquid expanded-like and liquid condensed-like phases for pure Insulin.

the  $K^s$  vs  $\Pi$  curve of insulin films in presence of  $\text{Zn}^{2+}$  exhibits a minimum at  $\sim 15$  mN/m. This minimum value of  $K^s$  increased as the proportion of egg-PC increased in the monolayers up to a value of 19.3 mN/m for the film of  $X_{\text{INS}} = 0.1$  while the monolayer collapse pressure decreased between the values of the pure Insulin and pure egg-PC. We previously described that Insulin  $\Pi_{\text{transition}}$  rises from 14.5 mN/m to 23.3 mN/m and from 14.5 to 15.5 when mixing with DPPC and POPC, respectively (Fig. 4). If we average the values of the  $\Pi_{\text{transition}}$  of Insulin at  $X_{\text{INS}} 0.05$  (23.3 and 15.5 for mixtures with DPPC and POPC, respectively) we also obtain 19.4 mN/m which coincides with the value reported by Perez-López et al. [32] using egg PC. Thus it is possible that the increase of the  $\Pi_{\text{transition}}$  of Insulin (strong evidence of a mixing process) in the mixed films with egg-PC at  $X_{\text{INS}} = 0.9$ – $0.95$  may be dominated by the DPPC component.

After Insulin reorganization, the Insulin-DPPC/POPC binary monolayers become more condensed, especially at high Insulin proportions in the film. This may also be due to the protein matrix bearing “molecular cavity” effects whereupon all or a part of one, usually the smaller, component molecules becomes “hidden” or trapped into surface cavities formed by the other in the mixture thus leading to apparent condensation as was found in binary mixtures of several lipids [27,12,26]. Such effects would be in agreement with entropy-driven effects in the Insulin-containing films (see below) and with calculations of the partial molar contribution to the mixture MMA and  $\Delta V_{\text{MMA}}$  of Insulin, DPPC and POPC at  $\Pi = 30$  mN/m (a surface pressure at which there are negative deviations from the ideal behavior at  $X_{\text{INS}} = 0.75$ – $0.25$ ; see Supplementary Fig. 1). The partial molar contributions of the lipids to the mixture MMA is decreased and reaches quite small, null or even negative values whereas those of Insulin remain rather linear and proportional to its mole fraction in the film. This suggests that

possible “molecular cavity” effects at high Insulin content ( $X_{\text{INS}} 0.75$ – $0.5$ ) may be mostly driven by a surface organization in which lipids become occluded in a protein-enriched lattice (it should be recalled that the minimum possible cross-sectional area of two closely packed hydrocarbon chains is about  $40 \text{\AA}^2/\text{molecule}$  for DPPC and about  $60 \text{\AA}^2/\text{molecule}$  for POPC). This may explain the deviations from ideality at high surface pressures and high Insulin proportion where the possibility of de-mixing is high. Nevertheless, it cannot be ruled out that changes of film molecular areas could also be due to changes in hexamer orientation when exposed to phospholipids.

### 3.2. Hysteresis of Insulin-DPPC/POPC Langmuir monolayers

The occurrence of hysteresis under consecutive film compression and expansion is a common phenomenon in Langmuir monolayers [5]. These effects arise from a balance among cohesion phenomena and viscoelastic properties of the interface that have different reversibility properties. This means that different molecular arrangements can be obtained depending on whether the energy and kinetic processes required for intermolecular cohesion upon compression are different to those involved in the molecular dispersion upon expansion [5]. Therefore, the presence of hysteresis is related to the meta-stability of closely packed states formed under compression and their tendency to slowly undergo reversible reorganization to an initial expanded state under expansion [4].

Fig. 6 shows that in films of pure DPPC, pure Insulin and all binary films of Insulin with DPPC and POPC exhibit some hysteresis (for the fully expanded pure films of POPC hysteresis is negligible). In the first compression–expansion cycle, the free energy change involved during compression is different to that released during

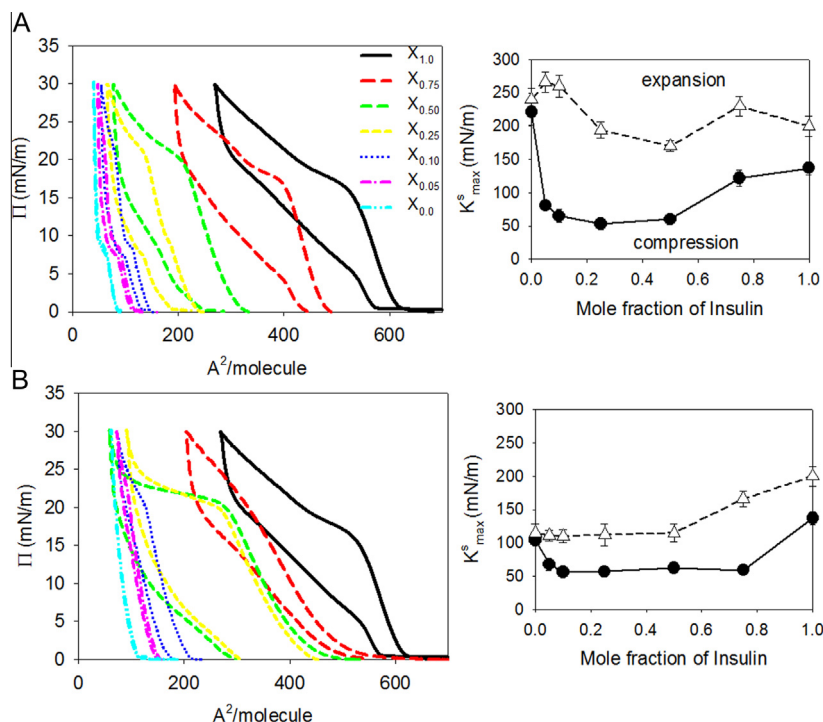


**Fig. 6.** (A) Hysteresis cycle of pure Insulin (black line), pure DPPC (cyan line) and their mixtures:  $X_{0.75}$  mole fraction of Insulin (red line),  $X_{0.5}$  (green line),  $X_{0.25}$  (yellow line),  $X_{0.1}$  (blue line) and  $X_{0.05}$  (pink line). Compression and expansion were performed at 24 °C at a speed of 20 Å<sup>2</sup>/molecule/min. Inset: maximum  $K^s$  values of pure components and their mixtures for compression and expansion isotherms. (B) Idem to A but for Insulin-POPC mixtures. (For interpretation of the references to color in this figure legend, the reader is referred to the web version of this article.)

**Table 1**

The free energy of compression ( $\Delta G_{\text{comp}}$ ), expansion ( $\Delta G_{\text{exp}}$ ), hysteresis ( $\Delta G^{\text{hys}}$ ), the configurational entropy of hysteresis ( $T\Delta S^{\text{hys}}$ ) and the enthalpy of hysteresis ( $\Delta H^{\text{hys}}$ ) calculated between  $\Pi = 1\text{--}30$  mN/m, for pure Insulins and DPPC-POPC and binary monolayers. All experiments were performed in triplicate and expressed as averages  $\pm$  SEM.

	$\Delta G_{\text{comp}}$ (kcal mol <sup>-1</sup> )	$\Delta G_{\text{exp}}$ (kcal mol <sup>-1</sup> )	$\Delta G^{\text{hys}}$ (kcal mol <sup>-1</sup> )	$T\Delta S$ (kcal mol <sup>-1</sup> )	$\Delta H$ (kcal mol <sup>-1</sup> )
<b>INS-DPPC</b>					
<i>1st cycle</i>					
$X_{1.00}$	4.66 $\pm$ 0.80	3.13 $\pm$ 0.04	-1.52 $\pm$ 0.04	-2.37 $\pm$ 0.20	-3.89 $\pm$ 0.24
$X_{0.75}$	4.22 $\pm$ 0.13	2.28 $\pm$ 0.22	-1.93 $\pm$ 0.35	-4.85 $\pm$ 0.08	-6.79 $\pm$ 0.43
$X_{0.50}$	3.66 $\pm$ 0.27	1.31 $\pm$ 0.09	-2.35 $\pm$ 0.17	-7.06 $\pm$ 1.20	-9.41 $\pm$ 1.30
$X_{0.25}$	3.39 $\pm$ 0.03	1.33 $\pm$ 0.09	-2.06 $\pm$ 0.05	-7.92 $\pm$ 0.79	-9.99 $\pm$ 0.85
$X_{0.10}$	0.92 $\pm$ 0.01	0.49 $\pm$ 0.01	-0.43 $\pm$ 0.02	-4.23 $\pm$ 0.35	-4.66 $\pm$ 0.37
$X_{0.05}$	0.51 $\pm$ 0.01	0.36 $\pm$ 0.01	-0.16 $\pm$ 0.01	-2.14 $\pm$ 0.17	-2.30 $\pm$ 0.19
$X_{0.00}$	0.34 $\pm$ 0.10	0.30 $\pm$ 0.09	-0.04 $\pm$ 0.01	-0.21 $\pm$ 0.03	-0.24 $\pm$ 0.03
<i>2nd cycle</i>					
$X_{1.00}$	4.38 $\pm$ 0.03	2.95 $\pm$ 0.05	-1.43 $\pm$ 0.08	-2.38 $\pm$ 0.09	-3.81 $\pm$ 0.17
$X_{0.75}$	4.12 $\pm$ 0.34	1.98 $\pm$ 0.17	-2.13 $\pm$ 0.51	-4.64 $\pm$ 0.31	-6.77 $\pm$ 0.82
$X_{0.50}$	2.76 $\pm$ 0.32	1.11 $\pm$ 0.05	-1.65 $\pm$ 0.27	-7.41 $\pm$ 0.80	-9.07 $\pm$ 0.70
$X_{0.25}$	2.62 $\pm$ 0.23	1.16 $\pm$ 0.08	-1.45 $\pm$ 0.14	-6.13 $\pm$ 0.24	-7.59 $\pm$ 0.09
$X_{0.10}$	0.78 $\pm$ 0.03	0.44 $\pm$ 0.01	-0.35 $\pm$ 0.03	-3.52 $\pm$ 0.17	-3.87 $\pm$ 0.20
$X_{0.05}$	0.50 $\pm$ 0.01	0.34 $\pm$ 0.01	-0.15 $\pm$ 0.02	-2.03 $\pm$ 0.14	-2.18 $\pm$ 0.13
$X_{0.00}$	0.33 $\pm$ 0.09	0.29 $\pm$ 0.09	-0.04 $\pm$ 0.01	-0.24 $\pm$ 0.02	-0.28 $\pm$ 0.01
<b>INS-POPC</b>					
<i>1st cycle</i>					
$X_{1.00}$	4.66 $\pm$ 0.80	3.13 $\pm$ 0.04	-1.52 $\pm$ 0.04	-2.37 $\pm$ 0.20	-3.89 $\pm$ 0.24
$X_{0.75}$	3.74 $\pm$ 0.27	2.20 $\pm$ 0.09	-1.54 $\pm$ 0.10	-3.42 $\pm$ 0.43	-4.96 $\pm$ 0.61
$X_{0.50}$	4.90 $\pm$ 0.09	1.77 $\pm$ 0.49	-3.12 $\pm$ 0.41	-13.49 $\pm$ 0.25	-16.62 $\pm$ 0.16
$X_{0.25}$	3.19 $\pm$ 0.18	1.69 $\pm$ 0.31	-2.22 $\pm$ 0.32	-7.51 $\pm$ 0.65	-9.73 $\pm$ 0.88
$X_{0.10}$	1.14 $\pm$ 0.13	0.73 $\pm$ 0.10	-0.42 $\pm$ 0.03	-3.20 $\pm$ 0.11	-3.63 $\pm$ 0.09
$X_{0.05}$	0.80 $\pm$ 0.03	0.63 $\pm$ 0.01	-0.17 $\pm$ 0.03	-1.29 $\pm$ 0.16	-1.46 $\pm$ 0.19
$X_{0.00}$	0.40 $\pm$ 0.01	0.37 $\pm$ 0.01	-0.03 $\pm$ 0.001	-0.10 $\pm$ 0.02	-0.12 $\pm$ 0.03
<i>2nd cycle</i>					
$X_{1.00}$	4.38 $\pm$ 0.03	2.95 $\pm$ 0.05	-1.43 $\pm$ 0.08	-2.38 $\pm$ 0.09	-3.81 $\pm$ 0.17
$X_{0.75}$	3.37 $\pm$ 0.19	2.16 $\pm$ 0.16	-1.22 $\pm$ 0.03	-3.24 $\pm$ 0.27	-4.45 $\pm$ 0.31
$X_{0.50}$	2.92 $\pm$ 0.08	1.19 $\pm$ 0.26	-1.73 $\pm$ 0.18	-11.44 $\pm$ 0.03	-13.17 $\pm$ 0.21
$X_{0.25}$	2.62 $\pm$ 0.14	1.40 $\pm$ 0.53	-1.22 $\pm$ 0.39	-5.30 $\pm$ 0.67	-6.52 $\pm$ 0.98
$X_{0.10}$	0.93 $\pm$ 0.12	0.65 $\pm$ 0.11	-0.28 $\pm$ 0.13	-2.47 $\pm$ 0.19	-2.74 $\pm$ 0.19
$X_{0.05}$	0.73 $\pm$ 0.01	0.63 $\pm$ 0.02	-0.10 $\pm$ 0.01	-0.81 $\pm$ 0.07	-0.91 $\pm$ 0.08
$X_{0.00}$	0.40 $\pm$ 0.01	0.38 $\pm$ 0.01	-0.03 $\pm$ 0.003	-0.14 $\pm$ 0.05	-0.16 $\pm$ 0.03



expansion, as reflected by the  $\Delta G_{\text{hys}}$  values shown in Table 1. This magnitude is indicative of the energy trapped as kinetically limited viscoelastic effects and/or cohesive intra- or intermolecular energies in the monolayer [5]. In the hysteresis cycle, the  $\Delta G^{\text{hys}}$  Insulin-DPPC ( $X_{\text{INS}} = 0.25\text{--}0.75$ ) and Insulin-POPC ( $X_{\text{INS}} = 0.75$ ) binary monolayers is considerably higher than that found for pure Insulin films. The negative values of  $\Delta G^{\text{hys}}$  indicate the retention of a considerable amount of free energy in the cycle.

The relatively large negative configurational entropy  $T\Delta S^{\text{hys}}$  observed in Insulin-DPPC ( $X_{\text{INS}} = 0.75\text{--}0.10$ ) and Insulin-POPC binary monolayers (Table 1) indicates the formation of entropically unfavorable, more compact and ordered molecular organizations. These states appear to be adopted under compression by the establishment of enthalpically favorable (exothermic) interactions, as revealed by the considerable negative enthalpy of hysteresis as calculated from the observed free energy and configurational entropy of hysteresis. The maximum values of  $K^{\text{s}}$  in films under compression and expansion (Fig. 6) clearly indicate that after compression the films remain in a stiffer arrangement under expansion. Such arrangements are more elastic in mixtures with DPPC than with POPC but, even for mixtures with this liquid expanded lipid, the  $K^{\text{s}}$  after the films have been compressed, remain significantly higher during expansion. For both lipids, the hysteresis shows a bimodal variation with the proportion of Insulin in the mixed films revealing maximum values for the thermodynamic parameters at protein mole fractions between  $X_{\text{INS}} = 0.25\text{--}0.75$ . This suggests preferable formation of composition-dependent packing arrangements at the interface. The similarities of the thermodynamics functions of hysteresis (Table 1) during the first and second cycles performed indicate the reproducibility of sequential hysteresis cycles.

### 3.3. Excess thermodynamics functions of Insulin-DPPC/POPC Langmuir monolayers

We analyzed the contribution to the excess free energy of mixing derived from the variation of the configurational entropy (Eqs. (6)–(11)) arising from changes of the MMA compared to ideal mixing behavior. Since, by definitions, in an ideally mixed monolayer intermolecular interactions are non-existent, the excess enthalpy is null, and the free energy of mixing is derived entirely from the entropy of mixing [5]. Fig. 7A and B shows the unfavorable (positive) excess compression free energy of mixing in Insulin-DPPC and Insulin-POPC binary films when packed up to 30 mN/m, respectively. Clearly, because a non-ideal mixing phenomenon was observed, there are enthalpic–entropic compensations in these mixtures that account for the sign and magnitude of the excess free energy of mixing, depending on the protein proportions. Unfavorable negative  $T\Delta S^{\text{exc}}$  values were observed for Insulin-DPPC mixtures. This event is consistent with the appearance of regular stripes, observed by BAM (see next section), and a hyperpolarization of the monolayers (strong positive deviation of  $\Delta V/n$  vs  $X_{\text{INS}}$ , Fig. 5). On the contrary, Insulin-POPC binary monolayers showed positive values of  $T\Delta S^{\text{exc}}$  indicating an increased configuration entropy in these films. The spontaneously unfavorable mixed films with DPPC (positive  $\Delta G^{\text{exc}}$ ) are mostly driven by the establishment of enthalpically favorable interactions (negative  $\Delta H^{\text{exc}}$ ) that are overcome by unfavorable molecular configurational ordering (larger and negative  $\Delta S^{\text{exc}}$ ). In films with POPC, both positive enthalpic (unfavorable) and entropic (favorable) contributions account for the positive values of  $\Delta G^{\text{exc}}$  (Fig. 7).

### 3.4. Surface topography (BAM) of Insulin-DPPC/POPC binary Langmuir monolayers

The microscopic visualization of the monolayer surface topography can provide a further characterization on a larger scale

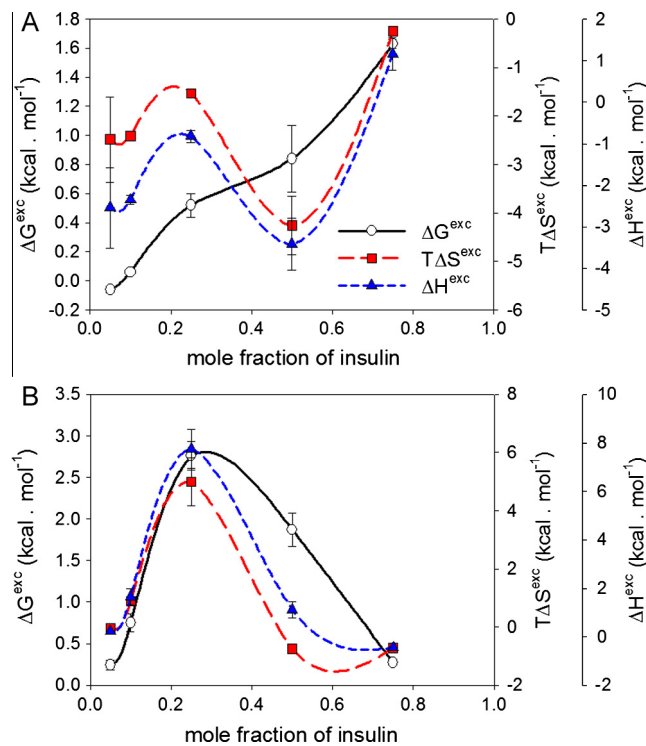


**Fig. 7.** (A) Excess thermodynamics functions of Insulin-DPPC binary monolayers. Data corresponds to calculated excess free energy of mixing (black line), excess entropy of mixing (red line) and excess enthalpy of mixing (blue line). All experiments were performed in triplicate; error bars =  $\pm$ SEM. (B) Idem A but for Insulin-POPC binary monolayers. (For interpretation of the references to color in this figure legend, the reader is referred to the web version of this article.)

[32]. We used BAM to visualize the monolayers. Figs. 8 and 9 show the surface micrographs of pure Insulin and DPPC and POPC monolayers and their mixtures at  $\Pi$  5–30 mN/m, respectively. A homogenous monolayer was observed for pure Insulin during the whole compression and at 5 mN/m for pure DPPC (Le phase) and its mixtures. Insulin-POPC binary films were also homogenous ( $X_{\text{INS}} = 0.75\text{--}0.05$ ) up to 15 mN/m. Such topography indicates miscibility on the micrometer scale; nothing can obviously be said for possible formation of clusters below the resolution limit of the BAM (about 2  $\mu\text{m}$ ), because if two components are immiscible in the surface film, spreading of a mixed solution will produce patches of one monolayer distributed in a monolayer of the other [19]. In pure DPPC monolayers at 10 mN/m we observed the classical condensed–expanded phase coexistence with triskelion-shaped domains and in films with  $X_{\text{INS}} = 0.05$  there are small round domains. Domain phase coexistence was observed in all binary monolayers at 20 mN/m. On the basis of the existence of deviations from the additivity rule for ideally mixed molecules in both MMA and  $\Delta V/n$  in the mixed films over certain proportions, together with lack of invariant collapse pressure of pure components, such domains should be due to immiscible phases formed by insulin–lipid mixtures in different proportions that become mutually segregated at defined mole fractions and surface pressures.

In films above 20 mN/m in mixtures with  $X_{\text{INS}} = 0.50$  and at 25–30 mN/m with  $X_{\text{INS}} = 0.75\text{--}0.5$  of Insulin we observed a 2D striped pattern. Above 20 mN/m in films with  $X_{\text{INS}} = 0.25$  of Insulin we observed the loss of stripes and the transition (from  $X_{\text{INS}} = 0.75$  to  $X_{\text{INS}} = 0.05$ ) to other supramolecular patterns. Similar phenomena were observed for Insulin-POPC binary monolayers at  $\Pi \geq 20$  mN/m. We found mostly two types of stripes: wide ones of  $\sim 30$   $\mu\text{m}$  length and thin ones of  $\sim 10$   $\mu\text{m}$  (Fig. 10). The wide ones appear to be an

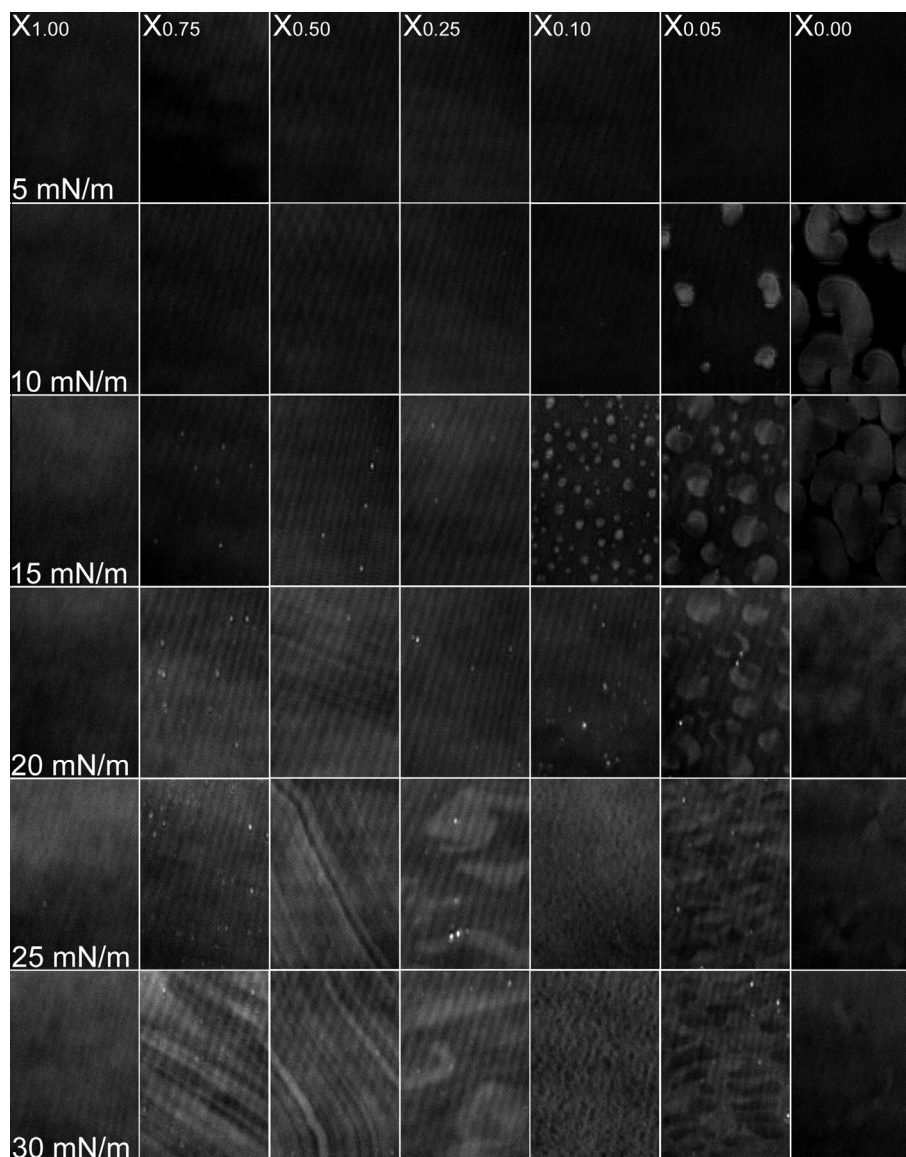


**Fig. 8.** BAM images of pure Insulin ( $X_1$ ), pure DPPC ( $X_0$ ) and their mixtures, at different surface pressures spread, on  $Zn^{2+}$  containing solution. For a better visualization the contrast of the images was enhanced from the original. Frame dimensions are  $185 \times 232 \mu\text{m}$ .

agglomeration of the thin ones. A pattern of stripes (if these were equilibrium structures) should be dominated by electrostatic repulsions over line tension [28,25]. Also, it should be taken into account that the appearance of stripes is associated with an increase of the film reflectivity (see Supplementary Fig. 2) and a decrease of  $\Pi_{\text{collapse}}$  (Figs. 1A and 4A). The collapse mechanism (2D-to-3D buckling or transition) involves complex effects related to pressure-induced defects in thin films [3]. All of our binary films collapsed at  $\Pi > 30 \text{ mN/m}$  (Figs. 1, 2 and 4) and the appearance of stripes at lower surface pressures might be related to some de-mixing process on approaching the collapse point (or to reversible collapse via folding/buckling of the monolayer).

Pérez-López et al. [32] showed that on  $Zn^{2+}$ -containing sub-phases, the two components in Insulin-egg PC films separate at the interface only at proportions of Insulin  $X_{\text{INS}} = 0.3\text{--}0.5$  and at surface pressures of  $\sim 30 \text{ mN/m}$ . Under such conditions, it was suggested that the protein may begin to form 3D fibril aggregates and fractures at the edges of pure Insulin domains [32]. A growing body of evidence suggests that formation of linearly ordered protein aggregates, generally called amyloids, is a common, generic feature

of proteins as polymers [33]. Insulin was proven to be a common model protein for studies on amyloidogenesis which easily forms amyloid like fibrils with  $\beta$ -pleated sheet structure and distinct staining properties [33]. The pattern of 3D aggregates shown by Pérez-López et al. [32] and by us, when pure Insulin is compressed at high pressures (see Supplementary Fig. 3), were very similar to those observed when Insulin is aggregated in bulk [33] suggesting the possibility of 3D fibril formation. In the presence of divalent cations, the protein and the egg PC molecules mixed at the interface over the whole monolayer compression only for films with the lowest Insulin mole fraction [32]. But when we used pure DPPC and POPC (the two major components of egg PC) we observed that Insulin mixes partially with the lipids, as described in the previous sections, and no 3D fibril aggregates were observed by BAM. However, it is important to remark that Pérez-López et al. mixed Insulin with egg PC two-dimensionally by spreading the protein onto a preformed lipid monolayer [32]. In our case, we spread both components in pre-mixed protein-lipid homogeneous solutions in a single solvent phase [18]. This could be responsible for the differences observed. Nevertheless, our results remain in agreement

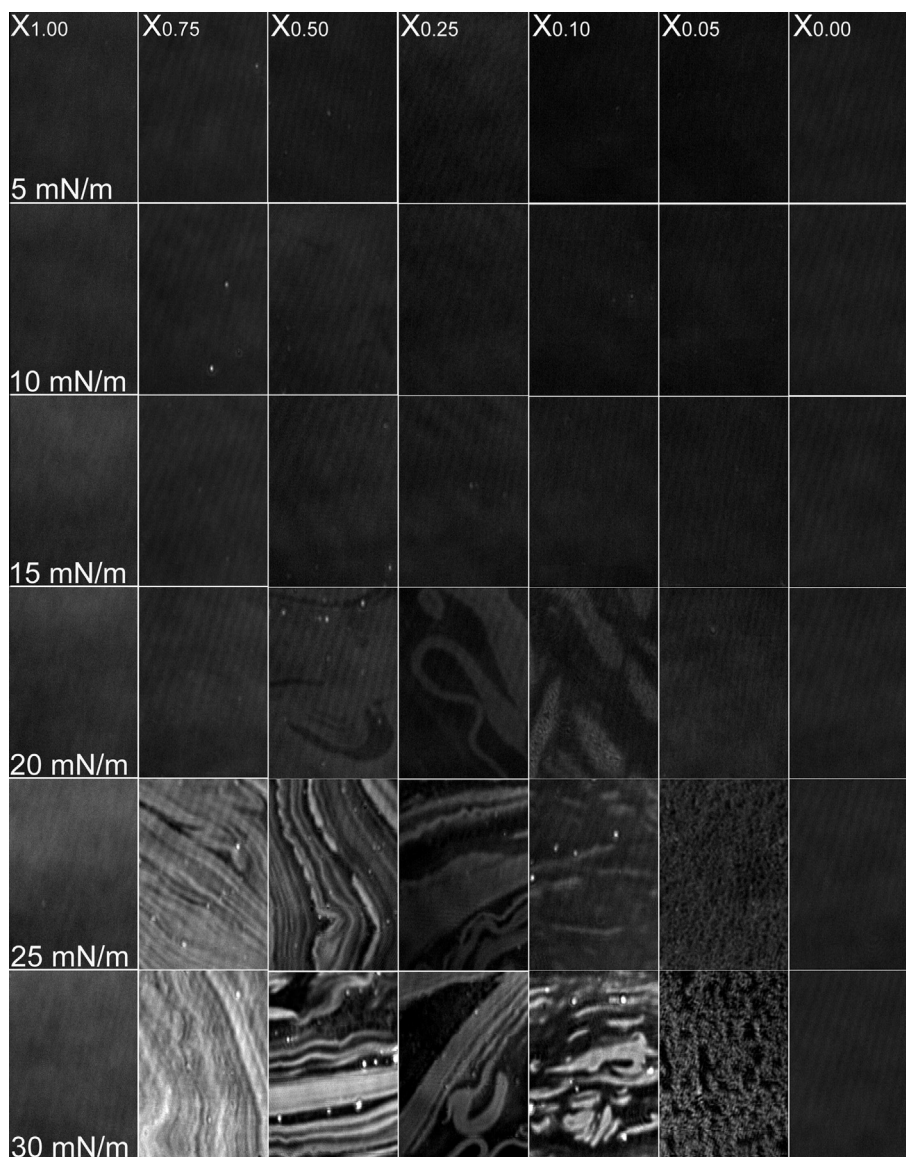


**Fig. 9.** BAM images of pure Insulin ( $X_1$ ), pure POPC ( $X_0$ ) and their mixtures, at different surface pressures spread, on  $Zn^{2+}$  containing solution. For a better visualization the contrast of the images was enhanced from the original. Frame dimensions are  $185 \times 232 \mu\text{m}$ .

with the proposal of those authors that above  $\sim 20$  mN/m the binary films may reach a de-mixing point over a range of composition.

As mentioned in Section 1, Insulin is prone to aggregation in aqueous solutions resulting in a huge complication for elaborating pharmacological formulations. Thus several efforts were made in order to develop new drug formulations for Insulin [11]. For instance, incorporation of Insulin into cubic phases of mono-olein results in the protein's unfolding and stability being influenced by confinement due to geometrical limitations, and vice versa, the topological properties of the lipid matrix can change as well [23]. Surprisingly, new cubic structures are induced by Insulin incorporation into the lipid matrix. When insulin begins to partially unfold at higher temperatures, the structure of the new cubic phase changed and finally disappeared at about  $60^\circ\text{C}$ , where an aggregation process sets in. The aggregation *in cubo* proceeds much faster and leads to the formation of medium-size oligomers or clusters, while the formation of large fibrillar agglomerates, as observed in bulk Insulin aggregation, is absent [23]. We found, as mentioned before, that near the collapse pressure of pure Insulin monolayers in presence of  $Zn^{2+}$  a pattern that might be interpreted as fibrillar [33] could be observed (see Supplementary Fig. 3).

However, we did not find such structures when mixing Insulin with DPPC or POPC at all mole fractions. Moreover, by hysteresis determinations we found that, below a surface pressure of 30 mN/m and although a phase segregation was observed, the system appears to be either in a reversible or, at least, in a thermodynamically trapped and long-lived metastable state.

#### 4. Conclusions

In the present work we studied the molecular packing, thermodynamics and surface topography of binary Langmuir monolayers of Insulin and DPPC or POPC at the air–water interface on  $Zn^{2+}$  containing solutions. Below 20 mN/m Insulin forms non-ideal, stable mixed films with DPPC and POPC at all mole fractions studied (with exception of  $X_{\text{INS}} = 0.05$   $X_{\text{DPPC}} = 0.95$ , where domain coexistence was observed at 10 mN/m). Above 20 mN/m, a phase segregation process occurred in all monolayers. These phases are likely formed by immiscible Insulin–lipid mixtures in different proportions because no squeezing out of pure components was observed.

Under compression the films exhibit a viscoelastic or kinetically trapped organization leading to considerable composition-

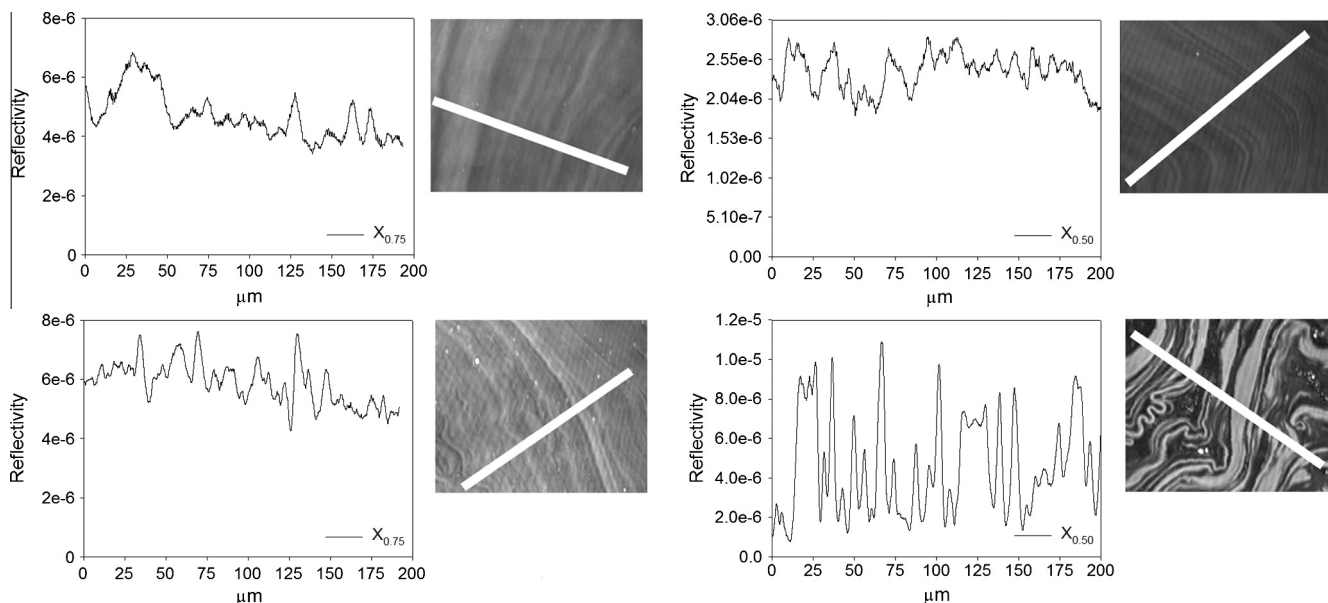


**Fig. 10.** Reflectivity as a function of distance in BAM images (indicated by the line in the pictures) at 30 mN/m. (A) Insulin-DPPC mix ( $X_{INS} = 0.75$ ), (B) Insulin-DPPC mix ( $X_{INS} = 0.5$ ), (C) Insulin-POPC mix ( $X_{INS} = 0.75$ ) and (D) Insulin-POPC mix ( $X_{INS} = 0.5$ ).

dependent hysteresis under expansion that occurs with entropic-enthalpic compensations. The unfavorable interactions of Insulin with DPPC are driven by favorable enthalpy that is overcome by unfavorable entropic ordering; in films with POPC both the enthalpic and entropic effects are unfavorable.

Our findings may be useful for future work as a basis for the construction of solid supported lipid-protein films for cellular growth in order to study the existence of sensitive transducing mechanisms involving the cell plasma membrane. As previously published [21], cultured neurons on supported pure insulin monomolecular films selectively respond to supramolecular signals at the film surface that appears to go beyond molecular specificity in the regulation of cellular function.

### Acknowledgements

This work was supported by grants from SECyT-UNC, FONCyT and CONICET, Argentina. E.J.G, R.G.O and B.M, are career investigators of CONICET.

### Appendix A. Supplementary material

Supplementary data associated with this article can be found, in the online version, at <http://dx.doi.org/10.1016/j.jcis.2015.11.034>.

### References

- [1] P.W. Atkins, *Physical Chemistry*, W. H. Freeman, New York, 1990 (Chapter 4).
- [2] A. Bellomio, R.G. Oliveira, B. Maggio, R.D. Morero, Penetration and interactions of the antimicrobial peptide, microcin J25, into uncharged phospholipid monolayers, *J. Colloid Interface Sci.* 285 (1) (2005) 118–124.
- [3] L. Benedini, M.L. Fanani, B. Maggio, N. Wilke, P. Messina, S. Palma, P. Schulz, Surface phase behavior and domain topography of ascorbyl palmitate monolayers, *Langmuir* 27 (17) (2011) 10914–10919.
- [4] K.S. Birdi, *Lipid and Biopolymer Monolayers at Liquid Interfaces*, Plenum Press, New York and London, 1989 (Chapter 5).
- [5] G.A. Borioli, B. Maggio, Surface thermodynamics reveals selective structural information storage capacity of c-Fos-phospholipid interactions, *Langmuir* 22 (4) (2006) 1775–1781.
- [6] J. Brange, U. Ribel, J.F. Hansen, G. Dodson, M.T. Hansen, S. Havelund, S.G. Melberg, F. Norris, K. Norris, L. Snel, et al., Monomeric insulins obtained by protein engineering and their medical implications, *Nature* 333 (6174) (1988) 679–682.
- [7] H. Brockman, Dipole potential of lipid membranes, *Chem. Phys. Lipids* 73 (1–2) (1994) 57–79.
- [8] H.L. Brockman, C.M. Jones, C.J. Schwebke, J.S. Smaby, D.E. Jarvis, Application of a microcomputer-controlled film balance system to collection and analysis of data from mixed monolayers, *J. Colloid Interface Sci.* 78 (2) (1980) 502–512.
- [9] R.E. Brown, H.L. Brockman, Using monomolecular films to characterize lipid lateral interactions, *Methods Mol. Biol.* 398 (2007) 41–58.
- [10] C. Bryant, D.B. Spencer, A. Miller, D.L. Bakaysa, K.S. McCune, S.R. Maple, A.H. Pekar, D.N. Brems, Acid stabilization of insulin, *Biochemistry* 32 (32) (1993) 8075–8082.
- [11] G.P. Carino, E. Mathiowitz, Oral insulin delivery, *Adv. Drug Delivery Rev.* 35 (1999) 249–257.
- [12] D.C. Carrer, B. Maggio, Transduction to self-assembly of molecular geometry and local interactions in mixtures of ceramides and ganglioside GM1, *Biochim. Biophys. Acta* 1514 (1) (2001) 87–99.
- [13] F. Chiti, C.M. Dobson, Protein misfolding, functional amyloid, and human disease, *Annu. Rev. Biochem.* 75 (2006) 333–366.
- [14] S.W. Cushman, L.J. Wardzala, I.A. Simpson, E. Karnieli, P.J. Hissin, T.J. Wheeler, P.C. Hinkle, L.B. Salans, Insulin-induced translocation of intracellular glucose transporters in the isolated rat adipose cell, *Fed. Proc.* 43 (8) (1984) 2251–2255.
- [15] G. Dodson, D. Steiner, The role of assembly in insulin's biosynthesis, *Curr. Opin. Struct. Biol.* 8 (2) (1998) 189–194.
- [16] M.F. Dunn, Zinc-ligand interactions modulate assembly and stability of the insulin hexamer – a review, *Biometals* 18 (4) (2005) 295–303.
- [17] P. Dynarowicz-Latka, K. Kita, Molecular interaction in mixed monolayers at the air/water interface, *Adv. Colloid Interface Sci.* 79 (1999) 1–17.
- [18] J. Folch, M. Lees, Sloane, G.H. Stanley, A simple method for the isolation and purification of total lipids from animal tissues, *J. Biol. Chem.* 226 (1) (1957) 497–509.
- [19] G.L.J. Gaines, *Insoluble Monolayers at Liquid-gas Interfaces*, Interscience Publishers, 1966, p. 136.
- [20] E.J. Grasso, R.G. Oliveira, B. Maggio, Rheological properties of regular insulin and aspart insulin Langmuir monolayers at the air/water interface. condensing effect of  $Zn^{2+}$  in the subphase, *Colloids Surf. B Biointerfaces* 115 (2014) 219–228.
- [21] E.J. Grasso, R.G. Oliveira, M. Oksdath, S. Quiroga, B. Maggio, Controlled lateral packing of insulin monolayers influences neuron polarization in solid-supported cultures, *Colloids Surf. B Biointerfaces* 107 (2013) 59–67.
- [22] T. Kono, F.W. Robinson, T.L. Blevins, O. Ezaki, Evidence that translocation of the glucose transport activity is the major mechanism of insulin action on glucose transport in fat cells, *J. Biol. Chem.* 257 (18) (1982) 10942–10947.
- [23] J. Kraineva, V. Smirnovas, R. Winter, Effects of lipid confinement on insulin stability and amyloid formation, *Langmuir* 23 (13) (2007) 7118–7126.
- [24] W. Liu, S. Johnson, M. Micic, J. Orbulescu, J. Whyte, A.R. Garcia, R.M. Leblanc, Study of the aggregation of human insulin Langmuir monolayer, *Langmuir* 28 (7) (2012) 3369–3377.
- [25] M. Lösche, P. Krüger, Morphology of Langmuir monolayer phases, *Morphol. Condensed Matter* 600 (2002) 152–171.
- [26] B. Maggio, Favorable and unfavorable lateral interactions of ceramide, neutral glycosphingolipids and gangliosides in mixed monolayers, *Chem. Phys. Lipids* 132 (2) (2004) 209–224.

- [27] B. Maggio, J.A. Lucy, Studies on mixed monolayers of phospholipids and fusogenic lipids, *Biochem. J.* 149 (3) (1975) 597–608.
- [28] H.M. McConnell, M. Vrljic, Liquid–liquid immiscibility in membranes, *Annu. Rev. Biophys. Biomol. Struct.* 32 (2003) 469–492.
- [29] M. Nieto-Suárez, N. Vila-Romeu, I. Prieto, Behaviour of insulin Langmuir monolayers at the air–water interface under various conditions, *Thin Solid Films* 516 (2008) 8873–8879.
- [30] D.R. Owens, New horizons–alternative routes for insulin therapy, *Nat. Rev. Drug Discovery* 1 (7) (2002) 529–540.
- [31] S. Pérez-López, N.M. Blanco-Vila, P. Dynarowicz-Lątka, Behavior of insulin–sphingomyelin mixed Langmuir monolayers spread at the air–water interface, *Colloids Surf. A* 321 (2008) 189–195.
- [32] S. Pérez-López, N.M. Blanco-Vila, N. Vila-Romeu, Bovine insulin-phosphatidylcholine mixed Langmuir monolayers: behavior at the air–water interface, *J. Phys. Chem. B* 115 (30) (2011) 9387–9394.
- [33] V. Smirnovas, R. Winter, T. Funck, W. Dzwolak, Protein amyloidogenesis in the context of volume fluctuations: a case study on insulin, *Chemphyschem* 7 (5) (2006) 1046–1049.
- [34] S.S. Sorensen, F. Christensen, T. Clausen, The relationship between the transport of glucose and cations across cell membranes in isolated tissues. X. Effect of glucose transport stimuli on the efflux of isotopically labelled calcium and 3-O-methylglucose from soleus muscles and epididymal fat pads of the rat, *Biochim. Biophys. Acta* 602 (2) (1980) 433–445.